



Novel cardiac magnetic resonance biomarkers: native T1 and extracellular volume myocardial mapping

Paola Maria Cannaò^{1*}, Luisa Altabella², Marcello Petrini¹, Marco Ali³,
Francesco Secchi⁴, and Francesco Sardanelli^{4,5}

¹Postgraduation School in Radiodiagnostics, Università degli Studi di Milano, Via Festa del Perdono 7, 20122 Milan, Italy

²Department of Medical Physics, San Raffaele Scientific Institute, Via Olgettina 60, 20132 Milan, Italy

³PhD Course in Integrative Biomedical Research, Università degli Studi di Milano, Via Mangiagalli 31, 20133 Milan, Italy

⁴Unit of Radiology, Research Hospital Policlinico San Donato, San Donato Milanese, 20097 Milan, Italy

⁵Department of Biomedical Sciences for Health, Università degli Studi di Milano, Via Morandi 30, San Donato Milanese, 20097 Milan, Italy

KEYWORDS

Myocardial fibrosis;
Cardiomyopathies cardiac;
Native T1 mapping;
Magnetic resonance;
Imaging biomarkers

Cardiac magnetic resonance (CMR) is a non-invasive diagnostic tool playing a key role in the assessment of cardiac morphology and function as well as in tissue characterization. Late gadolinium enhancement is a fundamental CMR technique for detecting focal or regional abnormalities such as scar tissue, replacement fibrosis, or inflammation using qualitative, semi-quantitative, or quantitative methods, but not allowing for evaluating the whole myocardium in the presence of diffuse disease. The novel T1 mapping approach permits a quantitative assessment of the entire myocardium providing a voxel-by-voxel map of native T1 relaxation time, obtained before the intravenous administration of gadolinium-based contrast material. Combining T1 data obtained before and after contrast injection, it is also possible to calculate the voxel-by-voxel extracellular volume (ECV), resulting in another myocardial parametric map. This article describes technical challenges and clinical perspectives of these two novel CMR biomarkers: myocardial native T1 and ECV mapping.

Introduction

The identification of biomarkers of pathologic processes is one major aim of biomedical research. This is also possible using imaging techniques that increase show high sensitivity, specificity, and reproducibility as well as the possibility to provide quantitative measures on a voxel-by-voxel basis within particular organs and tissues. This represents a challenge both for technologists and clinicians.

In particular, a predictor for adverse cardiac outcome is diffuse fibrosis, due to an increase of collagen deposition, that can lead to an abnormal myocardial stiffness and contraction and finally to heart failure. For these reasons, the evaluation and quantification of diffuse fibrosis represent

an interesting biomarker of several cardiac diseases, with the potential for early diagnosis and prognostic value.^{1,2}

In the past, the detection of this collagen deposition was possible only invasively throughout myocardial biopsy. More recently, the capability of cardiac magnetic resonance (CMR) to non-invasively characterize different soft tissues allowed for reliably discriminating fibrotic from normal myocardium. Late gadolinium enhancement (LGE) is a well-established CMR technique widely used to evaluate ischaemic and non-ischaemic myocardial diseases, being the standard of care for detecting non-invasively scar tissue and replacement fibrosis.³

Nevertheless, LGE has several limitations. First of all, it is not a quantitative technique: signal intensity is measured using arbitrary units. These data could be normalized according to an internal or external reference, but the procedure is difficult and not always reproducible, a heavy

* Corresponding author. Tel: +39 0252774642, Fax: +39 0252774925, Email: paola.m.canna@gmail.com

limitation when longitudinal studies are under consideration. All in all, the LGE technique is incapable to provide useful information about diffuse pathological processes. In fact, the typical LGE findings are based on the difference between pathological myocardium and the remaining 'normal' myocardium whose signal is 'nulled' (in practice, strongly decreased) by special radiofrequency 'inversion' pulses at the beginning of the dedicated CMR sequence. As a consequence, the signal intensity of this apparently normal myocardium is strongly determined by the variable effect of nulling pulses, creating great difficulties for normalization and standardization. As a matter of fact, interstitial fibrosis commonly shows no regional scarring on images acquired for LGE and is often missed using this standard approach.⁴

In the past years, T1 mapping has been recognized as the elective non-invasive method to quantify diffuse myocardial fibrosis.² It provides parametric maps representing T1 values (in milliseconds) on a voxel-by-voxel basis. In order to overcome some intrinsic remaining limitations of this approach, the estimation of extracellular volume (ECV) fraction after intravenous administration of a gadolinium-based contrast material is emerging as an accurate biomarker in many cardiac diseases associated with diffuse myocardial fibrosis.⁵ Myocardial ECV represents the percentage of tissue volume corresponding to the extracellular space, which increases in the presence of diffuse fibrosis.⁶

Several studies underlined the importance of ECV imaging by CMR as a tool for visualizing and quantifying both focal and diffuse myocardial fibrosis due to either ischaemic or non-ischaemic origin.⁷ The use of novel quantitative parameters such as native T1 and ECV can facilitate diagnosis and prognosis of these conditions and can lead to a personalized therapy planning.⁷ This article describes technical challenges and clinical perspectives of these two novel CMR biomarkers: myocardial native T1 and ECV mapping.

Technical considerations

Each biological tissue has a specific T1 relaxation time based on its cellular and interstitial components. The technical protocol for T1 mapping requires a series of images using different inversion times to derive a T1 recovery curve resulting in a map that describes the relaxation value on a pixel-by-pixel (i.e. voxel-by-voxel) basis, expressed in milliseconds. In fact, a fundamental principle of MR imaging is that the signal intensity is based on the relaxation of hydrogen nuclei protons contained in each voxel (mainly those of the water and fat), when the patient body is positioned within a strong homogenous static magnetic field and irradiated with radiofrequency pulses approximating the Larmor frequency, i.e. the physical condition for the 'resonance'.⁸

Several post-processing software may be used to perform curve fitting of the data and calculate a T1 time for each voxel. Examples of images generated from one unenhanced and one contrast-enhanced T1 mapping sequences are shown in *Figures 1* and *2* respectively. Epicardial and endocardial contours or regions of interest (ROIs) within the left ventricular myocardium (carefully excluding the blood pool as well as the epicardial fat) are drawn to measure average myocardial T1 times (*Figure 3*). Of course, contrast-enhanced images are essential for the calculation of ECV. A dedicated software is used to perform three-parameter curve fitting of the data, and T1 relaxation time is displayed on a voxel-by-voxel basis, as a parametric image.

Multiple technical approaches are currently available to obtain a T1 mapping study, all of them derived from an electrocardiographically gated inversion-recovery (IR) sequence, including the Look-Locker (LL) sequence, the modified LL inversion-recovery (MOLLI) sequence, and the shortened MOLLI (ShMOLLI) sequence.

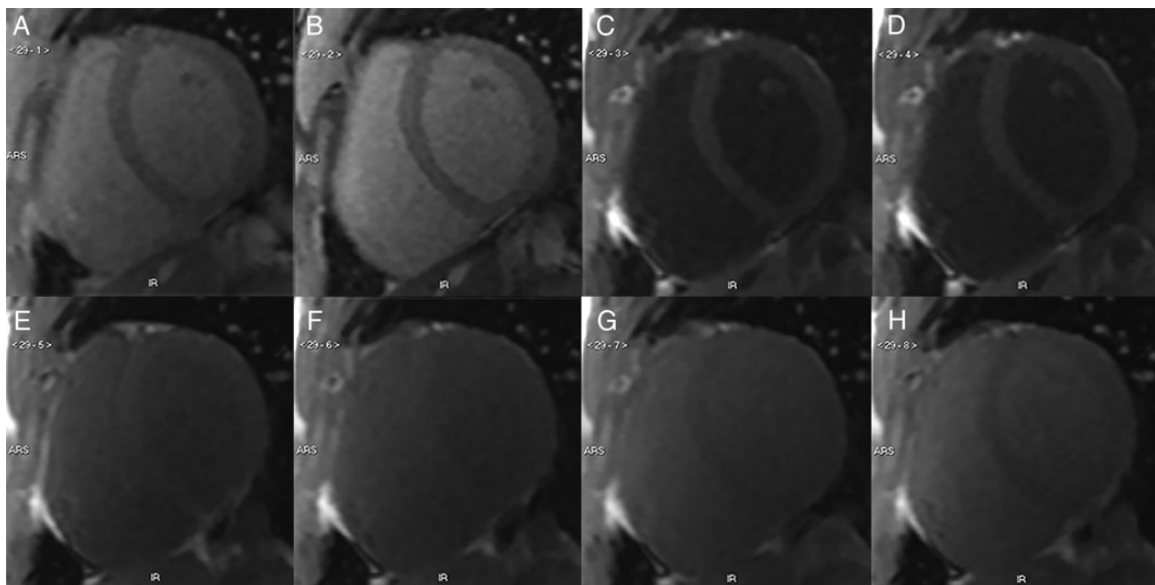


Figure 1 Native (i.e. unenhanced) short-axis T1-weighted acquisition of a healthy subject using a MOLLI sequence at 1.5T (Magnetom Aera, Siemens Medical Solutions, Erlangen, Germany): inversion time increases progressively from 100 ms (A) to 2675 ms (H). Note how the signal intensity of myocardium and blood changes according to the inversion time.

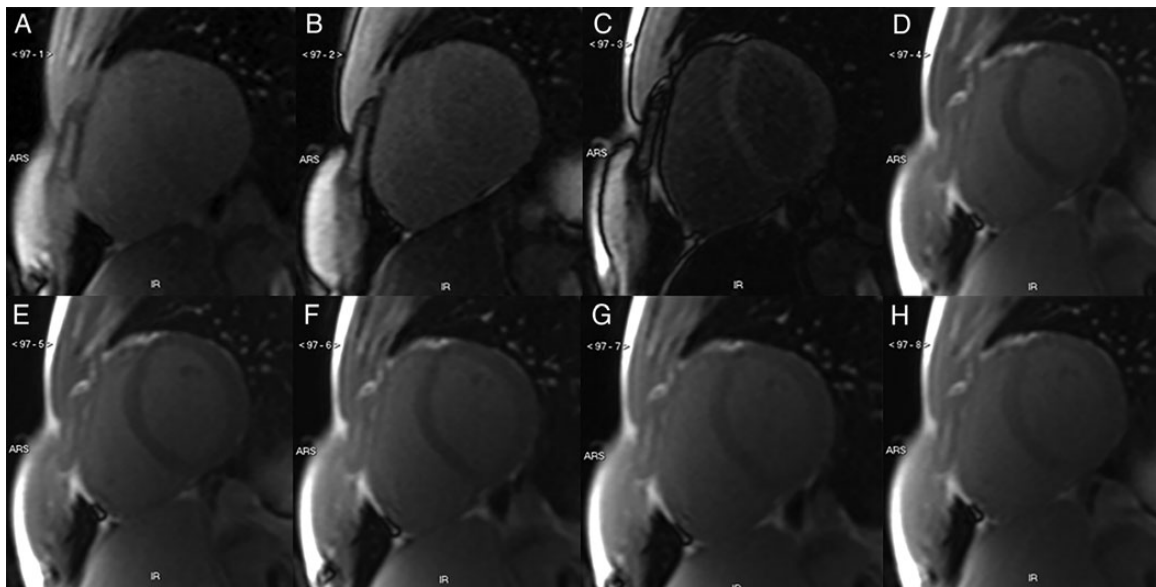


Figure 2 T1-weighted short-axis images of a healthy subject using a MOLLI sequence as in *Figure 1*, 15 min after intravenous injection of 0.1 mmol/kg of Gadobutrol (Bayer Pharma AG, Berlin): inversion time increases progressively from 100 ms (A) to 2675 ms (H). Note how the signal intensity of myocardium and blood changes according to the inversion time. If compared with *Figure 1*, the signal intensities of both myocardium and blood are generally higher as an effect of the reduction in T1 relaxation time due to the interaction between the paramagnetic Gd^{+++} and the water molecules.

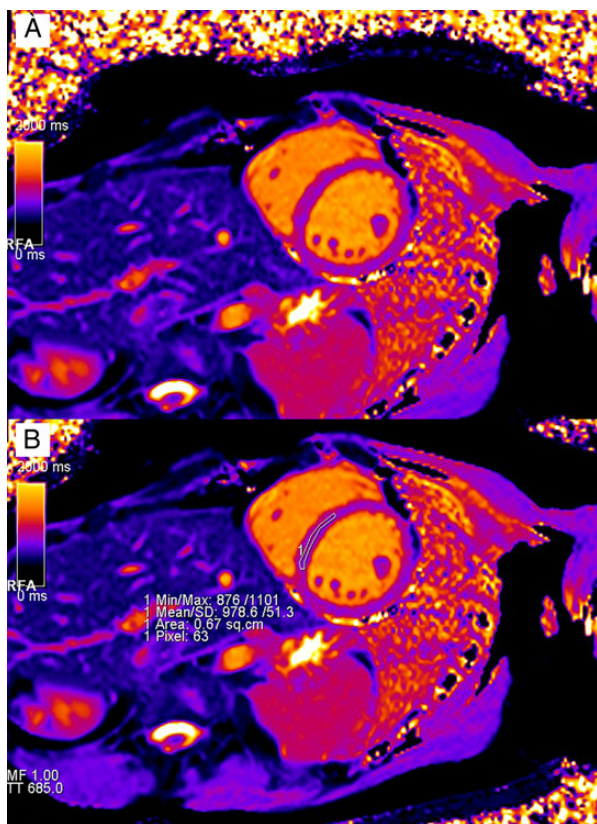


Figure 3 A native colour-coded T1 map generated from the original images shown in *Figure 1*. A ROI of 0.67 cm² drawn within the interventricular septum reveals that the T1 relaxation time of myocardium is 978 ± 51 ms (mean \pm standard deviation), in the range of normal values. On left side, the colorimetric scale spans from 0 to 2000 ms.

The LL sequence is composed of a series of ~ 20 images, which are usually acquired in a routine CMR examination to select the appropriate inversion time that nulls the myocardial signal (usually from 200 to 300 ms) for LGE studies. These images can be post-processed in order to provide a voxel-by-voxel map of T1 values.^{9,10} Major limitations are due to the variability of heart rate and the fact that the acquisition of images at different phase of the cardiac cycle is not allowed with this sequence.

The MOLLI sequence is a variant of the LL sequence. Images can be acquired from three consecutive IR pulses into one data set, generating single-slice T1 maps of the myocardium¹⁰ and the data are acquired at a fixed point in the cardiac cycle during 17 breath-hold heart beats for each T1 map slice.⁹ However, the accuracy of voxel-by-voxel T1 estimation could be compromised by the myocardial motion between frames, mainly due to beat-to-beat variation and respiration. For this reasons motion correction algorithms have been developed.⁹ Compared with LL sequence, MOLLI results to be shorter and significantly less burdened by errors correlated with the variability of the cardiac cycle phase.^{10,11}

A short breath-hold sequence represents an important goal especially for patients with pulmonary disease and a low heart rate. In order to reach this relevant aim, Piechnik *et al.*¹² described the ShMOLLI sequence, which requires a breath-hold of lasting 9.1 s; data acquisition is performed during 9 and not 17 heartbeats as is for the MOLLI sequence. They also demonstrated that ShMOLLI provide a T1 map in good agreement with that obtained with MOLLI sequences.¹²

Of note, these sequences led to an underestimation of the real T1 myocardial values by up about 30% due to several factors such as T2 dependence, magnetization

transfer effect, and dependence on the inversion pulse efficiency.¹³

Recently, other sequences for T1 mapping were introduced such as saturation recovery single-shot acquisition (SASHA) and saturation pulse prepared heart-rate-independent inversion recovery (SAPHIRE). The SASHA sequence can be performed in a single 10-heartbeat breath-hold; its accuracy is independent of absolute T1, heart rate, and flip angle, but it has lower precision compared with MOLLI.¹³ SAPHIRE sequences use a magnetization preparation obtained with pulses of saturation and inversion to create a T1 map with an increased dynamic range, but they are still inaccurate to assess native T1 values if compared with MOLLI.^{13,14}

Native T1 mapping

The native T1 is obtained without administration of contrast material using the previously described sequences. Native T1 reflects a composite of both intra- and extracellular compartments.¹⁵ It depends on different physiologic factors and technical parameters. For instance, myocardial T1 is longer at 3 Tesla than at 1.5 Tesla with an average increase by 28%.¹⁶

Normal native myocardial T1 values at 1.5 T using the MOLLI sequence are reported to be from 900 and 1100 ms.¹⁶ Increased or decreased T1 values in comparison with this normal range were observed in several myocardial diseases, showing a potential for T1 mapping in clinical diagnostics.

Several authors demonstrated an increased T1 native value in the case of *oedema related to acute infarction*, as a consequence of an increased water content resulting from cellular destruction and surrounding interstitial oedema, lasting up to 1 or 2 months after acute infarction.¹⁷ Oedema-related T1 elevation was demonstrated to provide a 90% sensitivity and specificity for the detection of acute myocardial infarction.^{18,19}

Others conditions related to the presence of myocardial oedema are myocarditis and Takotsubo syndrome, in which increased T1 relaxation times can be observed. In *myocarditis*, increased focal native T1 is co-localized with regions of LGE.²⁰ In *Takotsubo syndrome*, in which LGE is infrequently found, increased T1 relaxation time is found in typical hypokinetic regions.²¹ Patients with myocarditis were evaluated in 5 studies, including a total of 403 patients.^{20,22-25} In most of these studies, a comparison of T1 maps with T2-weighted imaging and LGE imaging was performed. Ferreira *et al.*²⁴ studied 50 patients and 45 controls: sensitivity of native T1 mapping resulted to be 91%, specificity 90%, when compared with the Lake Louise criteria. Luetkens *et al.*²⁵ found a 92% sensitivity associated to an 80% specificity for the same comparison. In a recent study of 60 patients, native T1 prolongation displayed the typical non-subendocardial non-ischaeamic patterns in acute myocarditis, similar to that obtained using LGE imaging but without the need for contrast material injection; using a threshold of T1 > 990 ms, they obtained a 90% sensitivity and an 80% specificity for the diagnosis of focal injury undetected by T2-weighted imaging and LGE.²⁰ Hinojar

*et al.*²² demonstrated that native T1 can reliably discriminate between healthy controls and patients as well as determine the disease stage in patients with a clinical diagnosis of myocarditis; native T1 mapping was superior to T2-weighted imaging and LGE, providing a very high diagnostic accuracy and positive and negative predictive values.

The native T1 mapping is more useful in the case of extracellular space expansion induced by diffuse fibrosis (e.g. interstitial fibrosis in *hypertrophic cardiomyopathy* and *dilated cardiomyopathy*), than by focal fibrosis (replacement fibrosis, infarction scar). In fact, focal lesions are assessable by both T1 mapping and LGE techniques. In contrast, in the case of diffuse, quite uniform T1 alterations, LGE is no longer able to depict abnormal patterns, since no relevant contrast is revealed between one region and another,¹⁶ while native T1 mapping can play a role as in the case of diffuse fibrosis.^{26,27}

Another disease in which native T1 has a great potential is *myocardial amyloidosis*, a restrictive cardiomyopathy due to infiltration of fibrillar proteins with a reduction of systolic function, diastolic dysfunction (*Figures 4 and 5*).²⁸ Karamitsos *et al.*²⁹ evaluated the utility of unenhanced T1 mapping using ShMOLLI sequences at 1.5 Tesla in patients with primary light-chain amyloidosis compared with normal controls. They found a native T1 threshold of 1020 ms resulting in a 92% accuracy for the diagnosis of cardiac amyloidosis. They also demonstrated how native T1 relaxation times correlated well with markers for systolic and diastolic dysfunction, reflecting the severity of cardiac involvement in these patients. Fontana *et al.*³⁰ studied 85 patients with transthyretin amyloidosis using ShMOLLI at 1.5 Tesla. They obtained an average native T1 value of 1097 ± 43 ms, slightly lower than of 1130 ± 68 ms in patients with light-chain amyloidosis. This differentiation may be clinically relevant in consideration of the different treatment and prognosis for each amyloidosis subtype.

The main causes of reduction in native T1 are intracellular sphingolipids overload (Anderson-Fabry disease) and iron overload. Sado *et al.*³¹ demonstrated a 9% reduction in native T1 septal relaxation time in patients with *Anderson-Fabry disease*, allowing for discrimination between this disease and several other causes of left ventricular hypertrophy, without overlap. Pica *et al.*³² demonstrated that in 50% of patients with the Anderson-Fabry disease without left ventricle hypertrophy myocardial T1 is reduced in association with echocardiographic parameters of cardiac dysfunction, suggesting that a lower T1 is a biomarker of early myocardial involvement.

A recent study demonstrated that LGE may underestimate the extension of fibrosis in patients affected with *hypertrophic cardiomyopathy*³³: a relatively lower native T1 value was measured in myocardial areas adjacent to LGE compared with that in remote areas. Puntmann *et al.*³⁴ demonstrated in 25 patients affected with hypertrophic cardiomyopathy and 25 patients with dilated cardiomyopathy that native T1 has a 100% sensitivity and a 96% specificity for this differentiation.

In the *cardiac iron overload* (e.g. in transfusion-dependent patients, mostly including *thalassaemia major*), a T1 reduction by ~14% strongly correlated with a reduction in T2* values.³⁵

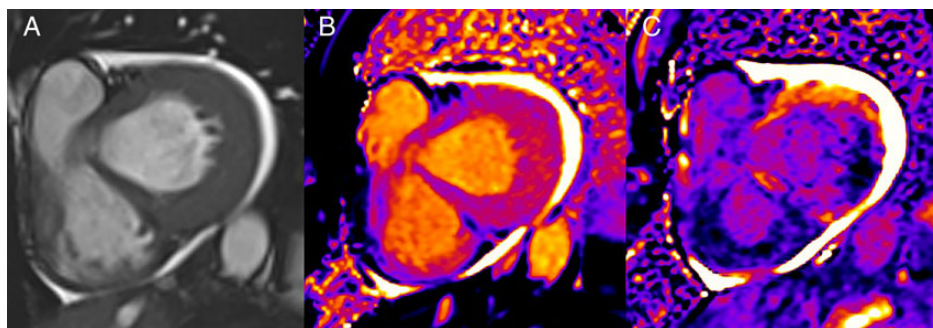


Figure 4 A 56-year-old male with left ventricle hypertrophy (amyloidosis). In (A), a short-axis, end-diastolic image showing a marked hypertrophy of the lateral wall. In (B), the native T1 map obtained with the MOLLI sequence showing higher and inhomogeneous T1 values of the hypertrophic lateral wall; conversely, the T1 map after injection 0.1 mmol/kg of Gadobutrol shows reduced signal intensity, as expected in the case of amyloid infiltration.

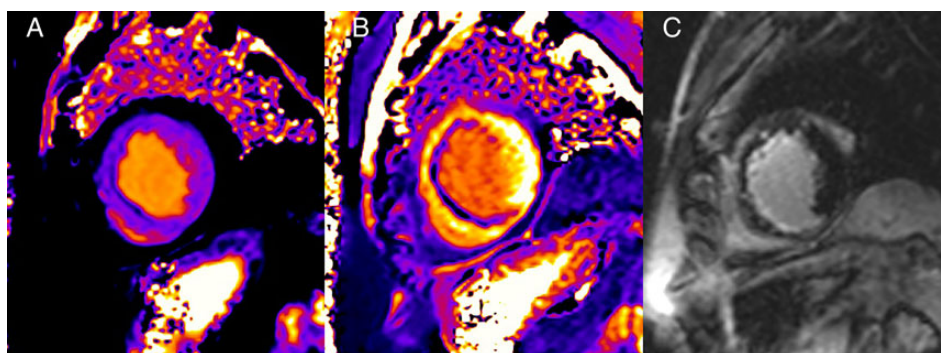


Figure 5 A 61-year-old male with chronic myocardial infarction. In (A), short-axis native T1 map (MOLLI sequence); in (B), same T1 map after injection of 0.1 mmol/kg Gadobutrol. Only in the T1 map after contrast (B), the infarct scar can be clearly differentiated from the blood pool as an elongated subendocardial area of reduction in T1 relaxation time. The finding is also visible in the usual inversion-recovery-prepared sequence of LGE (C). However, the conspicuity and the extension of the scar are better appreciated in the T1 map (B).

Mapping of extracellular volume fraction

Diffuse fibrosis implies the expansion of ECV. As a consequence, the biodistribution of two-compartment (intravascular/interstitial) extracellular contrast materials is locally influenced in tissues affected with diffuse fibrosis. Of note, the measurement of myocardial T1 after the intravenous administration of an extracellular contrast material implies several factors to be considered such as the injected dose, heart rate, gadolinium chelate clearance, time of measurement after injection, and haematocrit.³⁶ For these reasons, a direct ECV measurement was proposed for detecting and quantifying diffuse myocardial fibrosis.³⁷ Several studies underlined the potential of this approach.^{6,38–40}

Extracellular volume estimation is based on the myocardial uptake of contrast material relative to blood, when the equilibrium with the contrast material concentration in the blood pool is achieved. More in detail, changes in relaxivity, which are proportional to contrast material concentration, are defined as follows:

$$\Delta R1 = \frac{1}{T1_{\text{post}}} - \frac{1}{T1_{\text{pre}}}$$

where $\Delta R1$ is the Δ relaxivity, $T1_{\text{post}}$ is the T1 after contrast injection, and $T1_{\text{pre}}$ is the T1 before contrast injection.

If the ratio of the contrast material concentration between myocardium and blood is in equilibrium or in dynamic equilibrium, then the constant between $\Delta R1$ and contrast agent concentration can be cancelled out and for myocardium and blood, we obtain:

$$\frac{\Delta R1_{\text{myo}}}{\Delta R1_{\text{blood}}} = \frac{CA_{\text{myo}}}{CA_{\text{blood}}}$$

where CA_{myo} and CA_{blood} represent the contrast material concentration in the myocardium and blood, respectively. This ratio represents the partition coefficient λ . To obtain myocardial ECV, the percentage of extracellular space in the myocardium, i.e. the partition coefficient, has to be corrected for the fraction composed of plasma using haematocrit.

Finally, myocardial ECV can be expressed as follows:

$$ECV_{\text{myo}}(\%) = (1 - \text{haematocrit}) \cdot \left(\frac{\Delta R1_{\text{myo}}}{\Delta R1_{\text{blood}}} \right)$$

Myocardial ECV is calculated starting from native and contrast-enhanced T1 values both in blood and myocardium. These values can be obtained drawing ROI within the myocardium and the blood pool of the native and contrast-enhanced T1 map, thus obtaining only local ECV information. As a consequence, several authors have developed software to obtain reliable ECV maps.³⁷

Co-registration between unenhanced and contrast-enhanced T1 maps represents a very important requirement for ECV map quality. In fact, the images to derive unenhanced and contrast-enhanced T1 maps are acquired at different times, at least the time necessary to reach the contrast material equilibrium between myocardium and blood. This can lead to a patient displacement that has to be corrected to avoid misregistration in ECV map. The complexity of this procedure depends intrinsically on the T1 mapping technique. While usual image co-registration techniques are based on similar image contrast, image series for T1 mapping have different contrast due to different inversion times, necessary to obtain the T1 relaxation curve. To avoid this problem, Kellman *et al.*³⁷ suggested to co-register the last images of unenhanced and contrast-enhanced series (i.e. the ones with the longest inversion time) that present a similar contrast because both are acquired at the end of the recovery curve. The non-rigid transformation between these two images can then apply to the unenhanced and contrast-enhanced T1 maps.

One of the most relevant aspects involving ECV measurement regards the achievement of contrast material equilibrium between blood and myocardium. In theory, the steady state should be obtained using a continuous infusion of contrast material during the scan, but this approach has some practical limitations that make the use of bolus injection a preferred solution. The reliability of achieving the steady state using only a bolus of contrast agent has been studied in several works,^{36,40} and no differences with continuous infusion have been reported. In particular, the Society of Cardiovascular Magnetic Resonance has recommended the bolus-only approach to ECV measurement as sufficient for most myocardial ECV applications.⁴¹ In detail, for the bolus-only approach, with a single time-point contrast-enhanced measurement, a 15 min minimum delay should be used for ECV measures in non-infarcted myocardium.

Myocardial ECV has a normal range between 20 and 30%, and it is altered in the presence of several myocardial pathologic conditions such as diffuse fibrosis, acute and chronic myocardial infarction, myocarditis, hypertrophic cardiomyopathy, and amyloidosis.^{37–40} In particular, in *hypertrophic cardiomyopathy*, mean ECV is found increased by 36% in chronic myocardial infarction by 69%.³⁷

Amyloidosis also affects the myocardial ECV: several authors reported a significant increase of ECV.^{37,43} In particular, as yet shown for native T1 values, ECV is sensitive to different amyloidosis subtypes: ECV is significantly higher (58 vs. 54%) in patients with transthyretin amyloidosis than in those with light-chain amyloidosis, reflecting the presence of a greater amount of amyloid.⁴³

Five studies concerned T1 mapping amyloidosis, for a total of 280 patients.^{29,30,43–45} Despite the diversity of these studies, as mentioned above, authors demonstrated that myocardial native T1 mapping provides a high diagnostic performance for both light-chain and transthyretin amyloidosis when each group of patients is compared against patients with left ventricle hypertrophy from different causes such as aortic stenosis and hypertrophic cardiomyopathy.^{30,44} Banypersad *et al.*⁴⁴ studied a group of 100 patients and found a correlation with current

markers of disease severity in cardiac light-chain amyloidosis, confirming the presence of an increased ECV also in early cardiac involvement and its progressive increase when the disease is established. An ECV >0.45 remained significantly associated with mortality (hazard ratio = 4.41, $P = 0.01$) in a multivariate Cox model including measures of systolic and diastolic functions and serum biomarkers. In another recent study, Barison *et al.*⁴⁵ also demonstrated the correlation between ECV and amyloidosis disease severity (correlation between ECV and left ventricle ejection fraction, wall thickness and diastolic function, as well as natriuretic peptide, and cardiac troponin). Using a cut-off of ECV >0.316 (corresponding at 95th percentile in normal subjects), they obtained a 79% sensitivity and a 97% specificity for discriminating patients affected with amyloidosis from controls.

Subclinical cardiac abnormalities are common in patients affected with *rheumatoid arthritis*, including focal and diffuse myocardial fibrosis and inflammation. A recent study by Ntusi *et al.*⁴⁶ showed that these patients present a significantly increased ECV (30%) when compared with controls. High agreement has been found between ECV values and histological measurements of collagen deposition in myocardial tissue with a R^2 varying from 0.69 and 0.90,⁴⁷ while isolated contrast-enhanced myocardial native T1 measurements did not represent a good candidate to assess the collagen deposition.⁴⁸

Importantly, unlike native T1 values, ECV is not altered in patients affected with the *Anderson-Fabry disease* compared with control subjects.⁴⁹

On the contrary, ECV can play a relevant role in detecting fibrosis: ECV was higher in hypertrophic left ventricle segments without LGE in patients affected with hypertrophic cardiomyopathy.⁵⁰

Conclusions

Novel CMR T1 mapping techniques allow for a quantitative assessment of diffuse myocardial disease, in terms of both native T1 and ECV, the latter obtained combining images acquired before and after contrast injection. Even if those techniques are not yet routinely used in clinical practice, they are promising tools for early detection and monitoring of progression of cardiomyopathies. Large studies are warranted for clarifying the clinical role of T1 mapping. A potential for also an important prognostic role of these CMR imaging biomarkers does exist.

Conflict of interest: none declared.

References

1. Leong DP, Madsen PL, Selvanayagam JB. Non-invasive evaluation of myocardial fibrosis: implications for the clinician. *Heart* 2010;**96**: 2016–2024.
2. Burt JR, Zimmerman SL, Kamel IR, Halushka M, Bluemke DA. Myocardial T1 mapping: techniques and potential applications. *Radiographics* 2014;**34**:377–395.
3. Vogel-Claussen J, Rochitte CE, Wu KC, Kamel IR, Foo TK, Lima JA, Bluemke DA. Delayed enhancement MR imaging: utility in myocardial assessment. *Radiographics* 2006;**26**:795–810.

4. Flett AS, Hayward MP, Ashworth MT, Hansen MS, Taylor AM, Elliott PM, McGregor C, Moon JC. Equilibrium contrast cardiovascular magnetic resonance for the measurement of diffuse myocardial fibrosis: preliminary validation in humans. *Circulation* 2010;122:138–144.
5. Kellman P, Hansen MS. T1-mapping in the heart: accuracy and precision. *J Cardiovasc Magn Reson* 2014;16:2.
6. Jellis C, Martin J, Narula J, Marwick TH. Assessment of nonischemic myocardial fibrosis. *J Am Coll Cardiol* 2010;56:89–97.
7. Ugander M, Oki AJ, Hsu LY, Kellman P, Greiser A, Aletras AH, Sibley CT, Chen MY, Bandettini WP, Arai AE. Extracellular volume imaging by magnetic resonance imaging provides insights into overt and sub-clinical myocardial pathology. *Eur Heart J* 2012;33:1268–1678.
8. Rodgers CT, Robson MD. Cardiovascular magnetic resonance: physics and terminology. *Prog Cardiovasc Dis* 2011;54:181–190.
9. Hamlin SA, Henry TS, Little BP, Lerakis S, Stillman AE. Mapping the future of cardiac MR imaging: case-based review of T1 and T2 mapping techniques. *Radiographics* 2014;34:1594–1611.
10. Nacif MS, Turkbey EB, Gai N, Nazarian S, van der Geest RJ, Noureldin RA, Sibley CT, Ugander M, Liu S, Arai AE, Lima JA, Bluemke DA. Myocardial T1 mapping with MRI: comparison of look-locker and MOLLI sequences. *J Magn Reson Imaging* 2011;34:1367–1373.
11. Messroghli DR, Radjenovic A, Kozierke S, Higgins DM, Sivananthan MU, Ridgway JP. Modified Look-Locker inversion recovery (MOLLI) for high-resolution T1 mapping of the heart. *Magn Reson Med* 2004;52:141–146.
12. Piechnik SK, Ferreira VM, Dall'Armellina E, Cochlin LE, Greiser A, Neubauer S, Robson MD. Shortened modified Look-Locker inversion recovery (ShMOLLI) for clinical myocardial T1-mapping at 1.5 and 3T within a 9 heartbeat breathhold. *J Cardiovasc Magn Reson* 2010;12:69.
13. Roujol S, Weingartner S, Foppa M, Chow K, Kawaji K, Ngo LH, Kellman P, Manning WJ, Thompson RB, Nezafat R. Accuracy, precision, and reproducibility of four T1 mapping sequences: a head-to-head comparison of MOLLI, ShMOLLI, SASHA, and SAPPHERE. *Radiology* 2014;272:683–689.
14. Weingartner S, Akcakaya M, Basha T, Kissinger KV, Goddu B, Berg S, Manning WJ, Nezafat R. Combined saturation/inversion recovery sequences for improved evaluation of scar and diffuse fibrosis in patients with arrhythmia or heart rate variability. *Magn Reson Med* 2014;71:1024–1034.
15. Dass S, Suttie JJ, Piechnik SK, Ferreira VM, Holloway CJ, Banerjee R, Mahmod M, Cochlin L, Karamitsos TD, Robson MD, Watkins H, Neubauer S. Myocardial tissue characterization using magnetic resonance noncontrast T1 mapping in hypertrophic and dilated cardiomyopathy. *Circ Cardiovasc Imaging* 2012;5:726–733.
16. Germain P, El Ghannudi S, Jeung MY, Ohlmann P, Epailly E, Roy C, Gangi A. Native T1 mapping of the heart—a pictorial review. *Clin Med Insights Cardiol* 2014;8:1–11.
17. Goldfarb JW, Arnold S, Han J. Recent myocardial infarction: assessment with unenhanced T1-weighted MR imaging. *Radiology* 2007;245:245–250.
18. h-Ici DO, Jeuthe S, Al-Wakeel N, Berger F, Kuehne T, Kozierke S, Messroghli DR. T1 mapping in ischaemic heart disease. *Eur Heart J Cardiovasc Imaging* 2014;15:597–602.
19. Messroghli DR, Walters K, Plein S, Sparrow P, Friedrich MG, Ridgway JP, Sivananthan MU. Myocardial T1 mapping: application to patients with acute and chronic myocardial infarction. *Magn Reson Med* 2007;58:34–40.
20. Ferreira VM, Piechnik SK, Dall'Armellina E, Karamitsos TD, Francis JM, Ntusi N, Holloway C, Choudhury RP, Kardos A, Robson MD, Friedrich MG, Neubauer S. Native T1-mapping detects the location, extent and patterns of acute myocarditis without the need for gadolinium contrast agents. *J Cardiovasc Magn Reson* 2014;16:36.
21. Thavendirathan P, Walls M, Giri S, Verhaert D, Rajagopalan S, Moore S, Simonetti OP, Raman SV. Improved detection of myocardial involvement in acute inflammatory cardiomyopathies using T2 mapping. *Circ Cardiovasc Imaging* 2012;5:102–110.
22. Hinojar R, Foote L, Arroyo Ucar E, Jackson T, Jabbour A, Yu CY, McCrohon J, Higgins DM, Carr-White G, Mayr M, Nagel E, Puntmann VO. Native T1 in discrimination of acute and convalescent stages in patients with clinical diagnosis of myocarditis: a proposed diagnostic algorithm using CMR. *JACC Cardiovasc Imaging* 2015;8:37–46.
23. Radunski UK, Lund GK, Stehning C, Schnackenburg B, Bohnen S, Adam G, Blankenberg S, Muellerleile K. CMR in patients with severe myocarditis: diagnostic value of quantitative tissue markers including extracellular volume imaging. *JACC Cardiovasc Imaging* 2014;7:667–675.
24. Ferreira VM, Piechnik SK, Dall'Armellina E, Karamitsos TD, Francis JM, Ntusi N, Holloway C, Choudhury RP, Kardos A, Robson MD, Friedrich MG, Neubauer S. T1 mapping for the diagnosis of acute myocarditis using CMR: comparison to T2-weighted and late gadolinium enhanced imaging. *JACC Cardiovasc Imaging* 2013;6:1048–1058.
25. Luetkens JA, Doerner J, Thomas DK, Dabir D, Gieseke J, Sprinkart AM, Fimmers R, Stehning C, Homs R, Schwab JO, Schild H, Naehle CP. Acute myocarditis: multiparametric cardiac MR imaging. *Radiology* 2014;273:383–392.
26. Jellis CL, Kwon DH. Myocardial T1 mapping: modalities and clinical applications. *Cardiovasc Diagn Ther* 2014;4:126–137.
27. Hwang SH, Choi BW. Advanced cardiac MR Imaging for myocardial characterization and quantification: T1 mapping. *Korean Circ J* 2013;43:1–6.
28. Edelman RR. Contrast-enhanced MR imaging of the heart: overview of the literature. *Radiology* 2004;232:653–668.
29. Karamitsos TD, Piechnik SK, Banypersad SM, Fontana M, Ntusi NB, Ferreira VM, Whelan CJ, Myerson SG, Robson MD, Hawkins PN, Neubauer S, Moon JC. Noncontrast T1 mapping for the diagnosis of cardiac amyloidosis. *JACC Cardiovasc Imaging* 2013;6:488–497.
30. Fontana M, Banypersad SM, Treibel TA, Maestrini V, Sado DM, White SK, Pica S, Castelletti S, Piechnik SK, Robson MD, Gilbertson JA, Rowczenio D, Hutt DF, Lachmann HJ, Wechalekar AD, Whelan CJ, Gillmore JD, Hawkins PN, Moon JC. Native T1 mapping in transthyretin amyloidosis. *JACC Cardiovasc Imaging* 2014;7:157–165.
31. Sado DM, White SK, Piechnik SK, Banypersad SM, Treibel T, Captur G, Fontana M, Maestrini V, Flett AS, Robson MD, Lachmann RH, Murphy E, Mehta A, Hughes D, Neubauer S, Elliott PM, Moon JC. Identification and assessment of Anderson-Fabry disease by cardiovascular magnetic resonance noncontrast myocardial T1 mapping. *Circ Cardiovasc Imaging* 2013;6:392–398.
32. Pica S, Sado DM, Maestrini V, Fontana M, White SK, Treibel T, Captur G, Anderson S, Piechnik SK, Robson MD, Lachmann RH, Murphy E, Mehta A, Hughes D, Kellman P, Elliott PM, Herrey AS, Moon JC. Reproducibility of native myocardial T1 mapping in the assessment of Fabry disease and its role in early detection of cardiac involvement by cardiovascular magnetic resonance. *J Cardiovasc Magn Reson* 2014;16:99.
33. Lu M, Zhao S, Yin G, Jiang S, Zhao T, Chen X, Tian L, Zhang Y, Wei Y, Liu Q, He Z, Xue H, An J, Shah S. T1 mapping for detection of left ventricular myocardial fibrosis in hypertrophic cardiomyopathy: a preliminary study. *Eur J Radiol* 2013;82:e225–e231.
34. Puntmann VO, Voigt T, Chen Z, Mayr M, Karim R, Rhode K, Pastor A, Carr-White G, Razavi R, Schaeffter T, Nagel E. Native T1 mapping in differentiation of normal myocardium from diffuse disease in hypertrophic and dilated cardiomyopathy. *JACC Cardiovasc Imaging* 2013;6:475–484.
35. Sado DM, Maestrini V, Piechnik SK, Banypersad SM, White SK, Flett AS, Robson MD, Neubauer S, Ariti C, Arai A, Kellman P, Yamamura J, Schoenagel BP, Shah F, Davis B, Trompeter S, Walker M, Porter J, Moon JC. Noncontrast myocardial T1 mapping using cardiovascular magnetic resonance for iron overload. *J Magn Reson Imaging* 2015;41:1505–1511.
36. Schelbert EB. Clinical benefits of T1 and ECV mapping. *Magnetom Flash* 2015;12–17.
37. Kellman P, Wilson JR, Xue H, Bandettini WP, Shanbhag SM, Druet KM, Ugander M, Arai AE. Extracellular volume fraction mapping in the myocardium, Part 2: initial clinical experience. *J Cardiovasc Magn Reson* 2012;14:64.
38. Arheden H, Saeed M, Higgins CB, Gao DW, Bremerich J, Wytenbach R, Dae MW, Wendland MF. Measurement of the distribution volume of gadopentetate dimeglumine at echo-planar MR imaging to quantify myocardial infarction: comparison with ^{99m}Tc-DTPA autoradiography in rats. *Radiology* 1999;211:698–708.
39. Sado DM, Flett AS, Moon JC. Novel imaging techniques for diffuse myocardial fibrosis. *Future Cardiol* 2011;7:643–650.
40. Kehr E, Sono M, Chugh SS, Jerosch-Herold M. Gadolinium-enhanced magnetic resonance imaging for detection and quantification of fibrosis in human myocardium in vitro. *Int J Cardiovasc Imaging* 2008;24:61–68.
41. White SK, Sado DM, Fontana M, Banypersad SM, Maestrini V, Flett AS, Piechnik SK, Robson MD, Hausenloy DJ, Sheikh AM, Hawkins PN, Moon JC. T1 mapping for myocardial extracellular volume measurement by CMR: bolus only versus primed infusion technique. *JACC Cardiovasc Imaging* 2013;6:955–962.

42. Moon JC, Messroghli DR, Kellman P, Piechnik SK, Robson MD, Ugander M, Gatehouse PD, Arai AE, Friedrich MG, Neubauer S, Schulz-Menger J, Schelbert EB. Myocardial T1 mapping and extracellular volume quantification: a Society for Cardiovascular Magnetic Resonance (SCMR) and CMR Working Group of the European Society of Cardiology consensus statement. *J Cardiovasc Magn Reson* 2013;15:92.
43. Brooks J, Kramer CM, Salerno M. Markedly increased volume of distribution of gadolinium in cardiac amyloidosis demonstrated by T1 mapping. *J Magn Reson Imaging* 2013;38:1591–1595.
44. Banyersad SM, Fontana M, Maestrini V, Sado DM, Captur G, Petrie A, Piechnik SK, Whelan CJ, Herrey AS, Gillmore JD, Lachmann HJ, Wechalekar AD, Hawkins PN, Moon JC. T1 mapping and survival in systemic light-chain amyloidosis. *Eur Heart J* 2015;36:244–251.
45. Barison A, Aquaro GD, Pugliese NR, Cappelli F, Chiappino S, Vergaro G, Mirizzi G, Todiere G, Passino C, Masci PG, Perfetto F, Emdin M. Measurement of myocardial amyloid deposition in systemic amyloidosis: insights from cardiovascular magnetic resonance imaging. *J Intern Med* 2015;277:605–614.
46. Ntusi NA, Piechnik SK, Francis JM, Ferreira VM, Matthews PM, Robson MD, Wordsworth PB, Neubauer S, Karamitsos TD. Diffuse myocardial fibrosis and inflammation in rheumatoid arthritis: Insights from CMR T1 mapping. *JACC Cardiovasc Imaging* 2015;8:526–536.
47. Miller CA, Naish JH, Bishop P, Coutts G, Clark D, Zhao S, Ray SG, Yonan N, Williams SG, Flett AS, Moon JC, Greiser A, Parker GJ, Schmitt M. Comprehensive validation of cardiovascular magnetic resonance techniques for the assessment of myocardial extracellular volume. *Circ Cardiovasc Imaging* 2013;6:373–383.
48. Miller CA, Naish JH, Bishop P, Coutts G, Clark D, Zhao S, Ray SG, Yonan N, Williams SG, Flett AS, Moon JC, Greiser A, Parker GJ, Schmitt M. Response to letter regarding article, “Comprehensive validation of cardiovascular magnetic resonance techniques for the assessment of myocardial extracellular volume”. *Circ Cardiovasc Imaging* 2013;6:e26–e27.
49. Sado DM, Flett AS, Banyersad SM, White SK, Maestrini V, Quarta G, Lachmann RH, Murphy E, Mehta A, Hughes DA, McKenna WJ, Taylor AM, Hausenloy DJ, Hawkins PN, Elliott PM, Moon JC. Cardiovascular magnetic resonance measurement of myocardial extracellular volume in health and disease. *Heart* 2012;98:1436–1441.
50. Brouwer WP, Baars EN, Germans T, de Boer K, Beek AM, van der Velden J, van Rossum AC, Hofman MB. In-vivo T1 cardiovascular magnetic resonance study of diffuse myocardial fibrosis in hypertrophic cardiomyopathy. *J Cardiovasc Magn Reson* 2014;16:28.